This article has been accepted for inclusion in a future issue of this journal. Content is final as presented, with the exception of pagination.

A Wearable Hand Tremor-Suppressing Glove Using PVC Gel-Based Actuators and Force Sensors

Chen Liu, Yan Wang, and Ketao Zhang, *Member, IEEE*

***Abstract*—Hand tremor significantly impairs daily activities, affecting the quality of life for millions worldwide. Compared to traditional invasive treatments, noninvasive wearable devices offer a promising, more convenient, and safer alternative but often struggle to balance tremor suppression efficacy, wearability, and comfort. This study presents a novel wearable hand tremor-suppressing orthosis glove integrating semi-active and active control schemes using flexible polyvinyl chloride gel-based actuators and sensors. The glove integrates first, self-sensing semi-active absorbers to detect and suppress wrist and finger tremors, second, active fingertip tremor absorbers to counteract fingertip tremor forces, and third, two types of flexible sensors (resistive strain sensors and capacitive force sensors) to ensure accurate detection whether the hand is trembling in the air or in contact with a surface. Simulations and experiments validate the glove's ability to suppress tremors across a wide frequency range (3–12 Hz), achieving a suppression ratio of up to 81.7% at the fingertips. Compared to state-of-the-art solutions, the glove achieves a superior suppression-per-power metric of 163.4%/W, while maintaining low weight (155 g) and flexibility, enhancing comfort and adaptability. This work advances wearable tremor suppression by integrating semi-active and active schemes, offering a noninvasive and effective solution for hand tremors.**

***Index Terms*—Absorber, hand tremor, orthosis, sensor.**

I. Introduction

HAND tremors are a common motor symptom that may occur as part of various neurological disorders, including Parkinson's disease and essential tremor [1], [2]. They significantly impair fine motor skills and reduce the quality of life for millions of individuals. This disorder manifests in varying forms and frequencies [3–12 Hz (clinically, pathological and physiological hand tremors generally occur within a frequency range of approximately 3–12 Hz, where Parkinsonian rest tremor appears around 3–6 Hz, essential tremor typically lies between 6 and 12 Hz, and physiological tremor is observed near 8–12 Hz)] [3], [4], [5], [6], making it particularly challenging to manage effectively [7]. While traditional treatment options, such as medication and surgical interventions, can provide relief, they are often associated with invasiveness, high costs, or undesirable side effects [3]. As a result, noninvasive wearable devices have gained attention as practical alternatives, offering the potential for real-time, personalized tremor suppression that seamlessly integrates into daily life [8], [9].

Despite their promise, existing wearable tremor suppression devices face several key challenges. One key challenge is achieving an optimal balance among suppression efficacy, wearability, and user comfort [8]. While effective in reducing tremors, rigid devices are often bulky and uncomfortable, discouraging extended use [10]. Conversely, flexible devices offer improved comfort and adaptability but frequently fall short in suppression performance, particularly when addressing the diverse frequency and amplitude ranges of tremors [11].

Wearable tremor suppression systems typically rely on one of three control schemes: passive, semi-active, or active vibration control [12], [13]. Passive control schemes, while straightforward and reliable, use preset damping parameters and lack the adaptability required to respond to varying tremor frequencies. Consequently, their performance is often limited in dynamic or unpredictable conditions [14]. In contrast, the semi-active control schemes are advantageous for their simplicity and energy efficiency, dynamically adjusting damping forces to suppress high-frequency tremors effectively [15]. Variable stiffness actuators (VSAs), a class of semi-active or active actuation mechanisms, have drawn increasing attention due to their capability to adapt mechanical impedance dynamically. VSAs can adjust stiffness, enabling effective absorption and suppression of tremors across a broad frequency range (typically 3–12 Hz). In addition, stiffness modulation preserves device compliance during voluntary movements, ensuring minimal interference with normal functional tasks, thus making VSAs particularly suitable for wearable tremor suppression devices [8]. Prior studies using variable stiffness designs—such as layer-jamming actuators [9] and controllable fluidic dampers [11]—have demonstrated improved adaptability to patient-specific tremor profiles, although

Received 15 June 2025; revised 4 November 2025; accepted 5 February 2026. Recommended by Technical Editor Y. Karayiannidis and Senior Editor S. Katsura. This work was supported in part by the Royal Society International Exchanges Cost Share award under Grant EC NSFC211324 and in part by the Innovate U.K. Award under Grant 10074371. *(Corresponding author: Chen Liu.)*

The authors are with the Centre for Advanced Robotics, Queen Mary University of London, E1 4NS London, U.K. (e-mail: chen.liu@qmul.ac.uk; exx569@qmul.ac.uk; ketao.zhang@qmul.ac.uk).

Color versions of one or more figures in this article are available at https://doi.org/10.1109/TMECH.2026.3663307.

Digital Object Identifier 10.1109/TMECH.2026.3663307

1083-4435 © 2026 IEEE. All rights reserved, including rights for text and data mining, and training of artificial intelligence and similar technologies. Personal use is permitted, but republication/redistribution requires IEEE permission. See https://www.ieee.org/publications/rights/index.html for more information.

Authorized licensed use limited to: Queen Mary University of London. Downloaded on February 28,2026 at 20:34:18 UTC from IEEE Xplore. Restrictions apply.

This article has been accepted for inclusion in a future issue of this journal. Content is final as presented, with the exception of pagination.

tradeoffs in speed, control complexity, or integration remain. On the other hand, active control schemes excel in precision and responsiveness, particularly for low-frequency tremors. Still, their force output is often insufficient due to the size and weight constraints of wearable formats [16], [17].

Given the complementary strengths of semi-active and active control schemes, integrating these two approaches within a single device could provide a more robust solution for tremor suppression. Such a hybrid system would combine the energy efficiency and wide frequency range effectiveness of semi-active schemes with the precision and low-frequency responsiveness of active control strategies. However, despite these theoretical advantages, no existing wearable tremor suppression system has implemented such an integration [8], [18]. In addition, integrating sensors into traditional vibration absorbers allows for real-time feedback and control, potentially reducing system complexity by eliminating the need for separate external sensing modules [19]. However, wearable tremor suppression devices with fully integrated sensor-actuator systems remain unavailable, particularly for addressing hand tremors [17]. This underscores the need to develop a flexible hand tremor orthotic system that seamlessly combines semi-active and active absorption schemes through the design of wearable absorbers with integrated sensors, which will offer a promising pathway to leverage the strengths of each approach. However, such integration presents significant technical challenges, including 1) *sensor integration:* developing sensors that are sensitive enough to detect subtle tremors while being lightweight, flexible, and robust under dynamic conditions [19]; 2) *real-time control:* synchronizing semi-active and active schemes to operate seamlessly, requiring precise feedback and actuation mechanisms [7], [20]; and 3) *wearability:* ensuring that the device remains lightweight and flexible [10]. To address these challenges and advance technologies that overcome the limitations of existing devices, a shift is required from conventional design paradigms by incorporating emerging technologies, such as flexible capacitive sensors and VSAs. This article examines how these innovations can be leveraged to develop a more effective wearable tremor suppression solution that addresses the complex demands of real-world applications.

By focusing on integrating flexible sensors and hybrid control schemes, this study aims to pave the way for future wearable tremor suppression devices. By developing an innovative hand tremor suppression glove, this work seeks to bridge the gap between user comfort and suppression efficacy. Specifically, this study proposes a novel wearable hand tremor-suppressing orthosis glove (WHTOG), which integrates semi-active and active control schemes using advanced PVC gel-based actuators [17], [21] and sensors [22]. This dual-control strategy is designed to leverage the strengths of both schemes while addressing their limitations through seamless integration. Key innovations (see Fig. 1) include 1) self-sensing semi-active absorbers (SSSAs): this article introduces, for the first time, SSSAs developed using electric self-sensing variable stiffness artificial muscles [21]. These absorbers detect tremors at the wrist and metacarpophalangeal (MCP) joints and dynamically adjust stiffness in real time to effectively suppress vibrations, 2) active fingertip

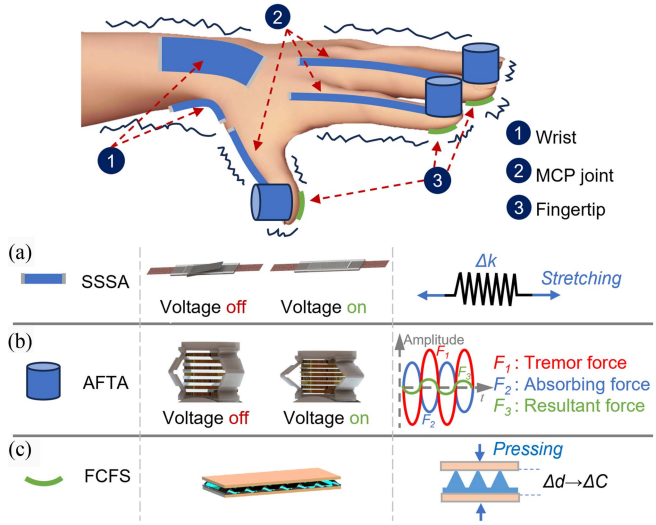

Fig. 1. Components of the WHTOG: (a) SSSAs detect tremors on the wrist and fingers by monitoring bending frequencies and increase stretching stiffness to provide damping forces at the wrist and MCP joints, (b) AFTAs generate vibration forces with the same frequency but opposite phase to counteract tremor forces, and (c) FCFSs are mounted on the fingertips to detect tremor forces during contact with surfaces.

tremor actuators (AFTAs): these actuators provide precise vibration control at the fingertips, generating opposite-phase and same-frequency forces to counteract residual tremors [17], and 3) two types of flexible sensors, including resistive strain sensors embedded in the SSSAs and flexible capacitive force sensors (FCFSs) [22] featuring microstructured PVC gel dielectric layers, ensure accurate tremor detection regardless of whether the hand is trembling freely in the air or in contact with a surface. The resistive strain sensors detect tremors by measuring strain-induced resistance changes, while the FCFSs provide high sensitivity and flexibility, enabling precise detection of small tremor forces when fingertips contact surfaces. This dual-sensor approach is particularly critical in scenarios where finger movement amplitudes are minimal, making it challenging for the SSSAs on the back of the fingers to detect tremors effectively.

By integrating these technologies, the WHTOG offers advancements in the field of wearable tremor suppression devices. It addresses the long-standing challenges of balancing efficacy and adaptability while enabling real-time, precise control of hand tremors. This innovation represents a step forward in improving the quality of life for individuals living with hand tremor-related disabilities.

II. Methods and Materials

A. Operational Procedure

The basic operational procedure of the WHTOG is illustrated in Fig. 2(a), where SSSAs and FCFSs detect tremors by frequency. If the detected frequency is less than 3 Hz, then it is classified as a normal intended finger action. In contrast, it is considered a tremor when the frequency is over or equal to 3 Hz. Then, the SSSA is triggered by the high voltage generated by the amplifier (Q10-5 DC, XP Power, U.K.). An SSSA is applied

Authorized licensed use limited to: Queen Mary University of London. Downloaded on February 28,2026 at 20:34:18 UTC from IEEE Xplore. Restrictions apply.

This article has been accepted for inclusion in a future issue of this journal. Content is final as presented, with the exception of pagination.

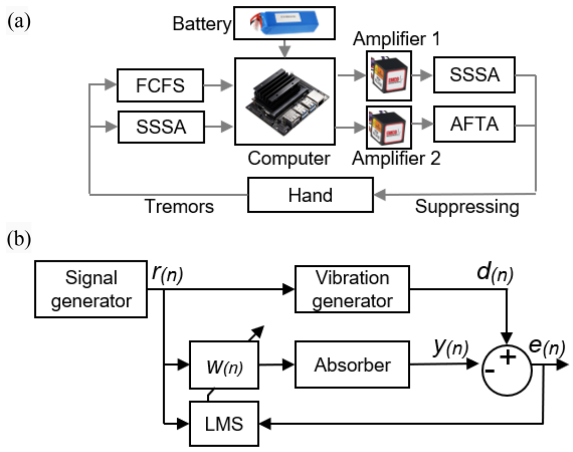

Fig. 2. Working logic of the WHTOG: (a) the operational process of the WHTOG, showcasing how SSSAs, AFTAs, and FCFSs coordinate for tremor detection and suppression and (b) the LMS algorithm utilized for active absorption, enabling precise counteraction of finger tremor forces.

with voltages to increase the stiffness and offer a damping force. In addition, via a least mean square (LMS) algorithm [23], which runs in the computer (Jetson Nano, NVIDIA Corporation, USA), the AFTA is also triggered by the high voltage generated by another amplifier to produce vibrations with the same frequency but opposite phase as the tremor to counteract the residual tremor forces on the fingertips.

The LMS algorithm is a common active vibration control method [24], which is applied for closed-loop control. The LMS algorithm is an adaptive algorithm that uses the gradient-based steepest descent method, as shown in Fig. 2(b). It adopts an estimate of the gradient vector from the available data [25], which is expressed as

$$w(n+1) = w(n) + \mu \cdot r(n) \cdot e(n) \tag{1}$$

where $w(n)$ and $w(n+1)$ are the weight vectors at point n and $(n+1)$, respectively [26]. $r(n)$ is the input reference signal vector (the tremor signal) stored in the filter-delayed line. μ is the convergence factor of the filter, and it can be obtained by the maximum eigenvalue of the autocorrelation function of the reference signal. $e(n)$ is the error signal (the residual vibration after the suppression detected by the SSSA or the FCFS) and can be described by

$$e(n) = d(n) - y(n) \tag{2}$$

where $d(n)$ is the desired signal (the vibration that happens on the finger before the suppression that is detected by the SSSA or the FCFS). $y(n)$ is the output signal (the vibration produced by the absorber) and is given by

$$y(n) = w(n) \cdot r(n)^T. \tag{3}$$

B. Incorporating Semi-active and Active PVC Gel-Based Absorbers

The PVC gel actuator utilizes the PVC gel's unique creeping property, as shown in Fig. 3(a). With the voltage ON, the PVC gel actively creeps toward the anode [27], resulting in the compression of the entire structure (cathode-PVC gel-anode mesh-PVC gel-cathode), as shown in Fig. 3(b). By stacking units in the arrangement of anode-PVC gel-cathode, the actuator can get the contract actuation over 12% of its thickness and can load over 78 kPa with a fast response of 0.1 ms [28].

An SSSA leverages artificial muscle technology [21] to achieve variable stiffness, enabling effective tremor suppression. It achieves variable stiffness by replacing the traditional rigid cathode with a stretchable cathode. When the voltage is OFF, the structure remains highly stretchable, as illustrated in Fig. 3(c). When the voltage is applied, the anode mesh of both sides absorbs the PVC gel with the cathode as anchors, resulting in reduced stretchability and increased stiffness. This variable stiffness mechanism allows the SSSA to deliver damping forces that adapt dynamically to tremor frequencies, making it suitable for wearable applications. Flexible artificial muscles in the form of PVC gel-based actuators enable the SSSA to combine flexibility and stiffness control, bridging the gap between comfort and functionality. The SSSAs are strategically positioned on the wrist (position 1) and the MCP joint (position 2), because the MCP joint is the most mobile among the finger joints, which is the most critical joint for suppressing finger tremors [29], [30], as shown in Fig. 1.

Complementing the SSSA is the active fingertip tremor absorber (AFTA), which addresses residual tremors that cannot be fully mitigated by semi-active damping. An AFTA is actuated by a stacked PVC gel actuator with multiple units. Each unit consists of three layers stacked in the sequence of the anode metal mesh-PVC gel layer-cathode (one anode layer, one gel layer, and one cathode layer) [see Fig. 3(d)]. It can absorb the PVC gel into the mesh, and the thickness of the actuator will decrease when applying the voltage to the anode [31], [32]. Based on the requirement that the dimensional area of the entire absorber should not exceed the width of the finger (average of 15 mm [33]) (two adjacent fingers will not affect each other when held together), the actuator is designed with a diameter of 14 mm. According to relevant studies [17], the number of stacked units is determined as 27, and the height and weight of the stacked actuator are measured as 19 mm and 12 g, respectively. The actuator is driven at up to 700 V over the 3–12 Hz range [4], [5], [34], corresponding to the frequency observed in tremors. It demonstrates that the stacked array generates approximately 1.03 mN of output force at 3 Hz. In the proposed system, the primary tremor forces reported in clinical studies to range up to 1 N at the fingertip during severe episodes [35], [36], [37] are first absorbed by the SSSAs, which provide structural damping at larger anatomical segments. This attenuates most of the mechanical energy transmitted to the distal phalanges. The AFTAs are therefore designed to fine-tune the suppression of residual tremors, whose amplitude and force fall well below clinical peak levels after upstream damping. Given their 1.03 mN output capacity, the AFTAs provide adequate correction for these localized, small-amplitude tremor components, particularly during light grasping or resting conditions. In addition, a 3D-printed Sarrus mechanism with flexure hinges as the exoskeleton [see Fig. 3(d)] to house the stacked PVC gel actuator without getting loose and can also minimize the swaying of the stacked linear actuator.

Authorized licensed use limited to: Queen Mary University of London. Downloaded on February 28,2026 at 20:34:18 UTC from IEEE Xplore. Restrictions apply.

This article has been accepted for inclusion in a future issue of this journal. Content is final as presented, with the exception of pagination.

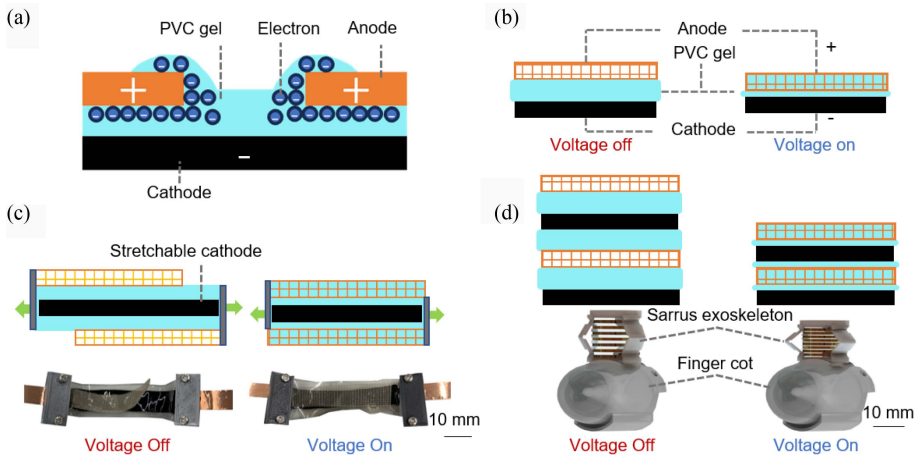

Fig. 3. Schematics of PVC gel-based absorbers: (a) the creeping phenomenon of the PVC gel actuator when voltage is applied, (b) schematic showing the actuation principle of a PVC gel actuator unit: applying voltage to the mesh, which absorbs the PVC gel and decreases the structure's thickness, (c) the variable stiffness principle of the SSSA, and (d) the actuation principle of the AFTA, featuring stacked PVC gel actuators within a Sarrus-mechanism exoskeleton.

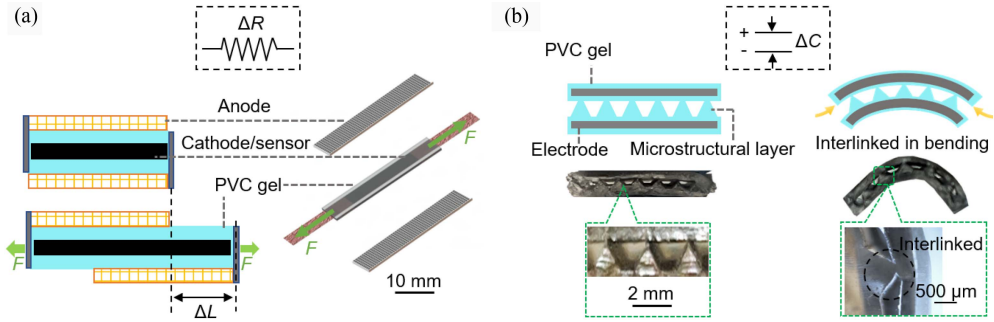

Fig. 4. Schematics of PVC gel-based sensors: (a) the resistive sensor embedded in the SSSA operates on the principle that resistance increases proportionally with the length of the sensor as it undergoes strain, enabling it to detect deformation accurately, and (b) the capacitive sensor FCFS, which maintains stable performance under bending due to its interlinked microstructural dielectric layer [22].

The incorporation of artificial muscles into the SSSA and AFTA represents a big step forward in wearable tremor suppression technologies. While the AFTA provides precise active control at the fingertips, the SSSA, with its artificial muscle-based stiffness control, serves as the primary absorber, addressing tremor forces at critical joints. Together, these absorbers form a hybrid system that combines the strengths of semi-active and active control schemes, offering a comprehensive and adaptive solution for hand tremor suppression. The placement of the SSSAs and AFTAs is determined based on anatomical and functional considerations. For the fingers, the SSSAs are positioned on the dorsal side to primarily address tremor forces occurring during finger extension, while preserving the palmar side for maintaining tactile sensitivity and minimizing interference with grasping tasks. In contrast, both dorsal and palmar placements are adopted for the palm and forearm regions to account for the more complex multidirectional tremor forces arising from larger muscle groups and joint movements in these areas. Finally, the AFTAs are strategically placed at the fingertip, where tremor amplitudes are typically amplified due to the kinematic chain effect [35], allowing for effective active suppression at the distal end of the finger.

C. PVC Gel-Based Sensors

While absorbers are applied to suppress hand tremors, sensors play a critical role in accurately detecting and monitoring these tremors. This article incorporates two types of PVC gel-based sensors to achieve comprehensive tremor detection: stretchable resistive strain sensors and FCFSs.

The stretchable resistive strain sensor, embedded in the SSSA as the cathode of the actuator, detects tremors by measuring strain-induced changes in electrical resistance, as shown in Fig. 4(a). As the sensor undergoes deformation, its resistance increases proportionally with the applied strain, providing real-time feedback on tremor amplitudes and frequencies [21]. This capability ensures effective tremor monitoring, particularly in scenarios involving dynamic hand movements.

The FCFSs, on the other hand, feature microstructured PVC gel dielectric layers, enabling high sensitivity and flexibility [22], as shown in Fig. 4(b). These sensors are mounted on the fingertips to detect small tremor forces when the hand is in contact with surfaces. Their precise detection capability complements the strain sensors, particularly in scenarios where finger movement amplitudes are minimal, making it difficult for

Authorized licensed use limited to: Queen Mary University of London. Downloaded on February 28,2026 at 20:34:18 UTC from IEEE Xplore. Restrictions apply.

This article has been accepted for inclusion in a future issue of this journal. Content is final as presented, with the exception of pagination.

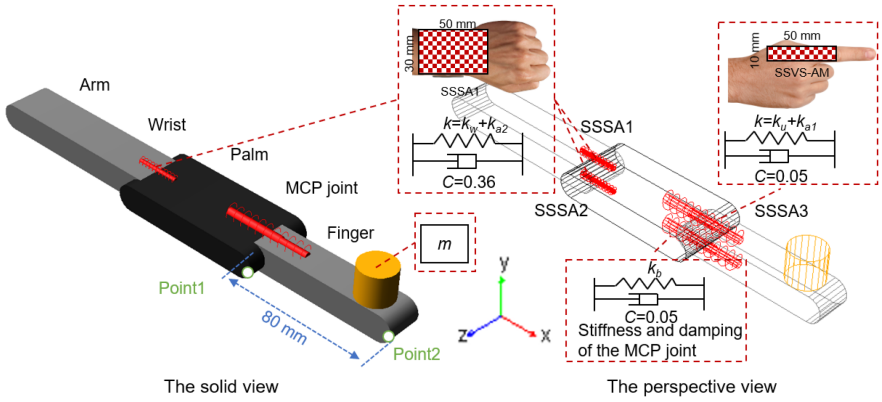

Fig. 5. Dynamic simulation settings: two SSSAs (SSSA1 and SSSA2) are mounted to the wrist, and another SSSA (SSSA3) is mounted on the MCP joints as spring–damping systems; an AFTA is mounted on the fingertip as a mass that can provide vibration forces.

the strain sensors on the back of the fingers to detect tremors effectively.

Both sensors operate by monitoring the frequency of hand movements to identify tremors, specifically targeting the typical tremor frequency range of 3–12 Hz [4], [5], [34]. Movements within this frequency range are classified as tremors, while frequencies below 3 Hz are considered normal intentional motions. This frequency-based monitoring enables accurate tremor detection in real time, allowing for effective activation of the absorbers to suppress tremors. By integrating these two types of sensors, this article demonstrates a hybrid sensing system that ensures precise tremor detection under various conditions, whether the hand is trembling freely in the air or interacting with objects. This dual-sensor approach enhances the overall performance and reliability of the wearable hand tremor suppression system.

III. Validations of the Concept

A. Dynamics Simulation

To get the theoretical performance of the new proposed WHTOG, dynamic simulations are conducted in ADAMS 2017, as shown in Fig. 5. Vibration forces along the y-axis direction are applied on the forearm to mimic hand tremors, and according to the classic theory for vibrations [38], the tremor force can be described as a simple harmonic force expressed as

$$F_0 = A_0 \sin(\omega t) \tag{4}$$

where F_0 is the tremor force, A_0 is the amplitude, ω is the tremor's angular velocity, and t is the time.

To verify the tremor suppression effect of the SSSAs, which are applied as semi-active tremor absorbers, a palm-wrist-hand and a palm-MCP joint-finger (see Fig. 5) tremor model are set up in the dynamic simulation software, ADAMS 2017 (MSC Software Corporation, USA), respectively . The weight of the palm with a finger is set as 0.5 kg, and the wrist is set as two spring–damper systems. The stiffness of each spring is $k = k_w(40\ \text{kN}\cdot\text{m}^{-1})+k_{a2}$ (the stiffness of the SSSA1/SSSA2 is $0.3\ \text{kN}\cdot\text{m}^{-1}$). The damping ratio C of each damper is 0.36 [39].

The stiffness and damping parameters used in the simulation are based on previous biomechanical studies and experimental characterizations. Specifically, the wrist joint stiffness ($k_w = 40\ \text{kN}\cdot\text{m}^{-1}$) is selected according to biomechanical literature [40]. The stiffness values for the SSSAs ($k_{a2} = 0.3\ \text{kN}\cdot\text{m}^{-1}$ and $k_{a2} = 0.1\ \text{kN}\cdot\text{m}^{-1}$) are determined experimentally through static tests on the fabricated PVC gel absorbers following previous procedures [21]. The damping ratio (C=0.36 for the wrist and C=0.05 for the MCP joint) is chosen based on literature and empirical measurements [41].

A vibration force (5 N) [36], [37] with different frequencies (between 3 and 12 Hz [4]) is set on the wrist to mimic tremors. Two SSSAs (SSSA1 and SSSA2) with a dimension of 50 mm × 30 mm are set on and under the wrist, as shown in Fig. 5. Unlike the wrist, the finger can only vibrate toward the palm due to the structure of the MCP joint [42]. Therefore, the MCP joint is set as two springs: the upper spring is $k = k_u(100\ \text{kN}\cdot\text{m}^{-1})+k_{a2}$ (the stiffness of the SSSA3 is $0.1\ \text{kN}\cdot\text{m}^{-1}$), and the bottom spring is $k_b = 10000\ \text{kN}\cdot\text{m}^{-1}$ and two dampers (the damping ratio C is 0.05) [43], [44]. The vibration force (1 mN) [4], [36], [37] with various frequencies (3–12 Hz) is set on the MCP joint to mimic tremors because the MCP joint is the most mobile among the finger joints, and it is the most critical joint for suppressing finger tremors [29], [45]. An SSSA3 with a dimension of 50 mm × 10 mm is set on the back of the finger and applied with 700 V voltage to increase the stiffness when the tremor occurs [21]. In addition, the weight of AFTA is set as 25 g as measured [17]. To semi-actively suppress tremors, SSSA1, SSSA2, and SSSA3 are actuated to increase the stiffness to 2.55 kN, 2.55 kN, and $0.85\ \text{kN}\cdot\text{m}^{-1}$, respectively. The AFTA on the fingertip is also triggered with a 700 V voltage to actively absorb residual tremors in responsive frequencies [17]. Point1 and Point2 are set as the measure points of the palm and the fingertip, respectively, to get the amplitude change along the y-axis, as shown in Fig. 5.

This work sets A_0 as 5 N, an average hand tremor force. The frequency of the vibration force varies between 3 and 12 Hz [3]. This simulation uses a simple harmonic excitation to approximate the dominant characteristics of tremor. Although real tremor signals may contain stochastic and nonlinear components, prior studies have shown that their main energy

Authorized licensed use limited to: Queen Mary University of London. Downloaded on February 28,2026 at 20:34:18 UTC from IEEE Xplore. Restrictions apply.

This article has been accepted for inclusion in a future issue of this journal. Content is final as presented, with the exception of pagination.

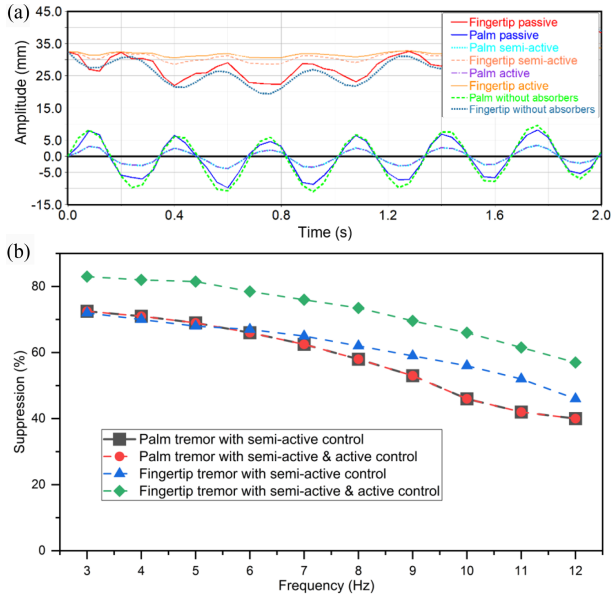

Fig. 6. Dynamic simulation results: (a) the result at 3 Hz and (b) results in different frequencies between 3 and 12 Hz.

is typically concentrated within a narrow frequency band (3–12 Hz) [35]. Therefore, a harmonic force provides a controlled and representative input to evaluate the absorber's response under typical tremor conditions [46]. This approach is commonly used in preliminary dynamic analyses for tremor suppression devices [47], [48]. Nevertheless, it is acknowledged that future models can be improved by incorporating recorded biological tremor signals to more accurately reflect real-world behavior. As shown in Fig. 6(a) under passive control (i.e., without absorbers actuation), the amplitude differences observed at the palm and fingertip between the baseline tremor condition (without the glove, bare hand) and the glove-wearing condition are both less than 1 mm at 3 Hz. This suggests that the glove introduces minimal mechanical impedance in its passive state and does not significantly interfere with natural hand motion. Although joint angle displacements are not directly measured, the fingertip displacement profiles and glove transparency suggest that joint motion is not constrained considerably during oscillation.

In this section, the tremor condition without any absorbers is treated as the baseline, against which the suppression performance of the semi-active (SSSA) and hybrid (SSSA + AFTA) modes is compared. The simulation results of the tremor amplitude at different frequencies are shown in Fig. 6. The condition without suppression serves as the original tremor input, and the results with different absorber combinations are compared against it. The result shows that with semi-active absorption, the tremor at 3 Hz on the palm and the finger can be attenuated effectively, and the amplitudes are reduced from 8 mm to 2.2 mm and from 6 mm to 1.68 mm, respectively, as shown in Fig. 6(a). After applying active absorption on the fingertip, the tremor of the finger can be further suppressed from 1.68 mm to 1.02 mm, while the suppression effect on the palm is almost the same as only semi-active absorption. This verifies that the AFTA can accurately affect the target object (the fingertip) in the spring and damping system without producing vibrations in other positions (the palm).

To get the numerical analysis of tremor suppression in various frequencies, this article conducts a series of dynamic simulations from 3 to 12 Hz under the same excitation amplitude ($A_0 = 5$ N), as shown in Fig. 6(b). The maximum damping forces produced by semi-active absorbers are 4.8 N (SSSA1 and SSSA2) and 1.6 N (SSSA3) for the wrist and the finger, respectively. The active absorber can provide a maximum vibration force of 1.03 mN for absorbing. The result indicates that semi-active absorption effectively reduces tremors at different frequencies in both the palm and the fingertip. According to the results, applying active absorption to the fingertip further suppresses tremors, while the tremors in the palm have not changed much. In addition, as the frequency varies from 3 to 12 Hz, the suppression ratio gets smaller. This is because the tremor force gets bigger when the frequency increases, while the maximum absorbing forces remain constant.

B. Experiments

1) Tests of Tremor Suppression: To further verify the hand tremor suppression effect of the WHTOG, this article designs a testing platform, as shown in Fig. 7(a). A vibration generator (1000701, 3B SCIENTIFIC PHYSICS, Germany) produces vibrations to mimic hand tremors, and the SSSA1 and the SSSA2 are affixed between the arm and the palm to detect and suppress tremors occurring on the wrist. In addition, the SSSA3 is affixed between the palm and the finger to detect and suppress tremors happening on the MCP joint of the finger. In addition, an AFTA is fixed on the fingertip to suppress the tremors of the finger actively. The testing platform is placed in the motion capture system (MOCAP) (OptiTrack, USA), operating at a sampling rate of 100 Hz. Three reflective markers are attached to the palm and the fingertip, respectively, to identify them as rigid bodies, which the MOCAP tracks. Each experimental trial lasted 60 s, and measurements were averaged over ten repeated trials to ensure reliability. Point1 and Point2 are set as the measure points of the palm and the fingertip, respectively, to get the amplitude change, as shown in Fig. 7(a). The testing devices are connected to Jetson Nano, which decouples the signal from the sensors (SSSAs and FCFSs). The test is also applied to use the LMS algorithm coded in Python, which sends the control signal (voltage) to absorbers via the amplifiers. In this study, a prosthetic hand is employed as a tremor simulation platform to validate the performance of the proposed wearable glove. The prosthetic hand used is a passive mechanical structure without active feedback control. The tremor-like oscillations in this study are mechanically induced via external vibration inputs, rather than by neuromuscular activations, which are responsible for generating tremors in human subjects. As a result, the dynamic behavior of the prosthetic hand differs from that of a biological hand, particularly in terms of joint stiffness and compliance. Specifically, the prosthetic joints exhibit substantially higher stiffness compared to human finger joints, which are typically characterized by low stiffness values (approximately 0.5–2.0 N · m/rad [44]) due to soft tissue elasticity and active neuromuscular control. Although the prosthetic platform does

Authorized licensed use limited to: Queen Mary University of London. Downloaded on February 28,2026 at 20:34:18 UTC from IEEE Xplore. Restrictions apply.

This article has been accepted for inclusion in a future issue of this journal. Content is final as presented, with the exception of pagination.

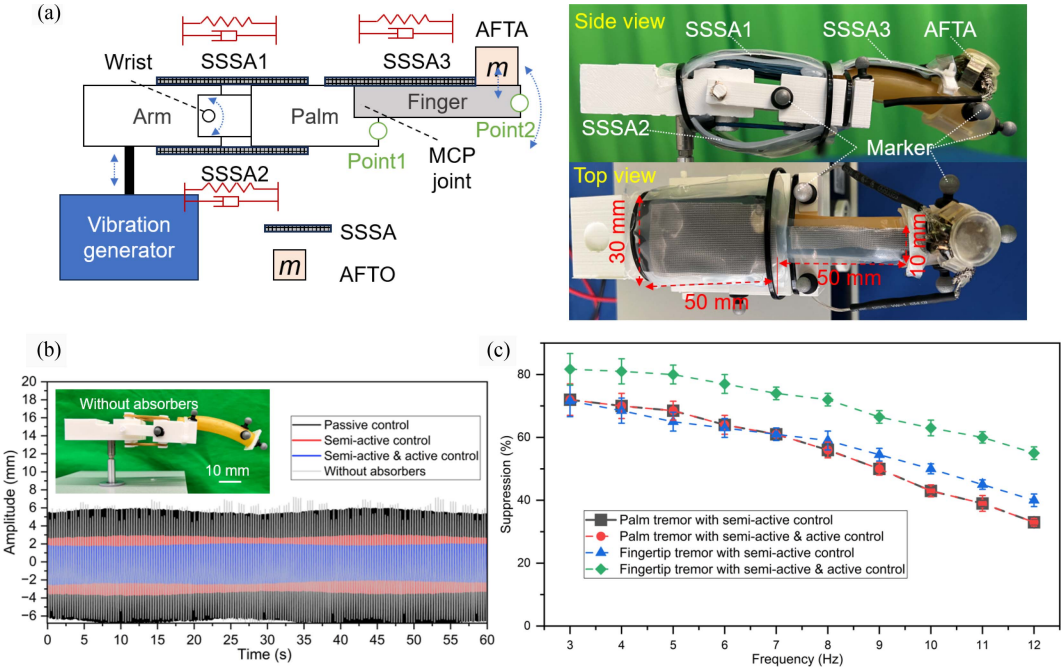

Fig. 7. Setting of the hand tremor suppression experiment platform in a MOCAP system and testing results. (a) Vibration generator produces vibrations to mimic hand tremors; SSSAs are attached to the wrist and the MCP joint to detect the tremor and produce damping forces to suppress tremors; an AFTA is fixed on the fingertip to produce vibration forces to suppress tremors. (b) Result of the tremor suppression on the fingertip experiment at 3 Hz in the time domain. (c) Experimental results of the palm and fingertip tremors suppression.

not replicate the complex neuromuscular dynamics of human tremors, it provides sufficient mechanical fidelity for evaluating the baseline performance of tremor suppression actuators in a controlled and repeatable manner. Future studies will aim to evaluate the system with human participants further to characterize tremor suppression performance fully under biological conditions.

The vibration generator produces vibrations between 3 and 12 Hz with the same amplitude of 10 mm. For instance, at 3 Hz, the measured fingertip displacement amplitude is 6.18 mm in the baseline condition (without the glove, bare hand) and 6.0 mm in the glove-wearing condition without absorbers activation. This small difference (<0.2 mm) demonstrates that the glove introduces minimal mechanical impedance in its passive state. Although joint angle displacements are not directly recorded in the experimental setup, the consistency in fingertip trajectories suggests that joint mobility is largely preserved. With the semi-active absorbers applied, as shown in Fig. 7(b), the tremor of the fingertip is suppressed to 1.7 mm (the suppression ratio is 71.6%). After the active absorber is applied, the tremor is further eliminated to 1.1 mm (the suppression ratio is 81.7%).

To ensure reliability and repeatability, the suppression results of the palm and fingertip tremors at each frequency are obtained from ten repeated trials, as presented in Fig. 7(c). The data trend in the test results closely matches that of the simulations. With semi-active vibration absorption, the palm's tremor suppression decreased from 72% to 37%, and the finger's tremor suppression dropped from 71.6% to 43% between 3 and 12 Hz. Following active vibration absorption, the palm's tremor suppression remains relatively stable, while the finger's tremor suppression is improved. Across the 3–12 Hz range, the finger's tremor suppression decreased from 81.7% to 62%.

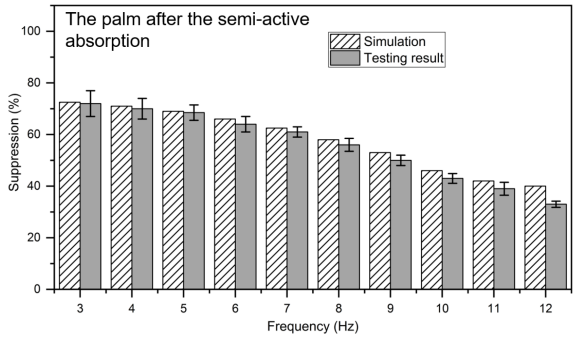

Fig. 8. Difference between the simulation and experiments of the palm after the semi-active absorption.

The average difference of 1.25% between the testing result and simulation of the palm and fingertip tremor semi-active suppression is shown in Fig. 8 and Fig. 9(a), respectively. This is due to the SSSAs being stretched when they are actuated to increase the stiffness after the detection of tremors, reducing the actuation areas of the SSSAs.

In addition, different from the simulation, the experimental results of the active fingertip tremor suppression are lower by an average of 1.04%, as shown in Fig. 9(b). The reason is that when the AFTA is actuated, its damping decreases, thereby diminishing the suppression effect. Although there are some differences between the experimental results and the simulation, they are generally consistent. This verifies the feasibility and working effect of the designed WHTOG.

Authorized licensed use limited to: Queen Mary University of London. Downloaded on February 28,2026 at 20:34:18 UTC from IEEE Xplore. Restrictions apply.

This article has been accepted for inclusion in a future issue of this journal. Content is final as presented, with the exception of pagination.

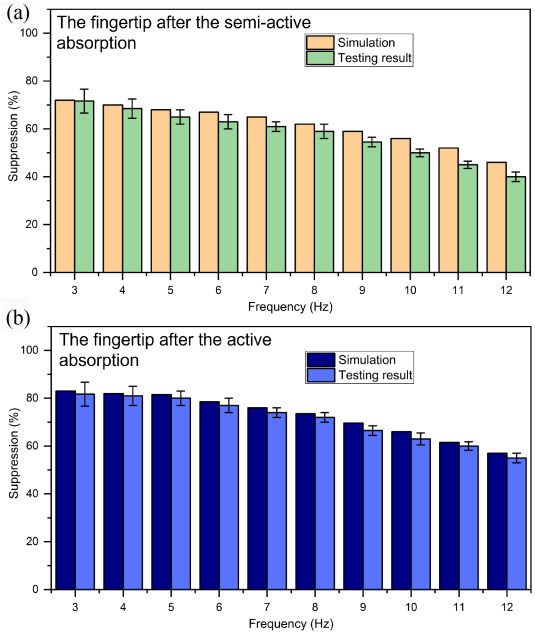

Fig. 9. Difference between the simulation and experiments of the fingertip after (a) the semi-active and (b) the active absorption.

2) Tests of Two Sensing Mechanisms: To evaluate the effectiveness of the two sensors (SSSA and FCFS) under various tremor conditions, three representative tremor scenarios are simulated: (a) resting tremor, the finger suspended freely without contact (baseline), (b) postural tremor with the fingertip supported by a rigid object, and (c) kinetic tremor during object holding. A frequency of 6 Hz is specifically chosen, as it is the most commonly observed tremor frequency in pathological hand tremors, providing a relevant benchmark for assessing sensor performance [3], [49]. In scenario (a), the finger is freely suspended in the air [see Fig. 10(a)]. Under this condition, the FCFS can hardly detect any force due to a lack of contact, whereas the SSSA successfully captures the vibration signals associated with finger tremors. After applying a second-order Butterworth bandpass filter (3–12 Hz), the dominant 6 Hz tremor component becomes clearly identifiable in the SSSA output. In scenario (b), simulating postural tremor when the finger maintains a static posture while touching a surface, the SSSA sensor detects minimal vibration due to the small amplitude of tremor motion at the fingertip–object interface [see Fig. 10(b)]. However, the FCFS sensor successfully captures subtle contact force variations induced by tremor, which, after the same bandpass filtering (3–12 Hz), clearly indicates the tremor frequency of 6 Hz. Scenario (c) simulates kinetic tremor during object holding [see Fig. 10(c)]. Here, a pair of magnets is used to clamp the fingertip gently, simulating a consistent grasping force measured by the FCFS, ensuring the object remains secured in the hand. Under this condition, the FCFS records the relatively constant grasp force while the SSSA effectively captures dynamic tremor signals. After filtering with the aforementioned Butterworth bandpass filter, the tremor was again confirmed at a 6 Hz frequency. These experiments demonstrate complementary sensing capabilities provided by combining the SSSA and FCFS sensors, effectively distinguishing between voluntary grasping actions and involuntary tremor movements.

3) Glove Prototype: The integration of the SSSA and AFTA control modules in the proposed glove system is implemented in a layered, decoupled manner. The semi-active SSSAs serve primarily as structural dampers that respond through voltage-controlled stiffness modulation without real-time signal dependency. In contrast, the AFTAs are controlled actively and precisely via a local LMS-based feedback loop, responding rapidly ($<$10 ms latency) to residual tremor frequencies. Given their differing response characteristics, anatomical placement, and actuation bandwidths, strict temporal synchronization is not required. Throughout all experiments conducted, no latency issues or dynamic conflicts between the two modules are observed. This decoupled yet complementary control architecture contributes significantly to system stability and ease of implementation.

Integrated with some fabric material and a 3D-printed resin attachment, the prototype of the WHTOG is developed in this work, as shown in Fig. 11. It consists of two SSSAs on the wrist, another three SSSAs on the thumb, the index finger, and the middle finger, and three AFTAs on each fingertip with the FCFSs. The Velcro straps at the wrist and the flexible perforated board on the back of the hand make the entire glove adaptable to different sizes of hands.

C. Comparison With Other Hand Tremor Suppression Orthoses

To validate the advancements and practical benefits of the proposed WHTOG, a comparative analysis with other representative hand tremor suppression devices is conducted (see Table I). Several critical factors, including absorbing schemes, substrates, weights, maximum suppression ratio, suppression-to-weight ratio (S/W), power consumption, and energy efficiency (E), are evaluated.

In terms of absorbing schemes, tremor suppression orthoses are typically categorized into passive, semi-active, and active types. Passive orthoses, such as the lightweight passive orthosis (33 g) by Fromme et al. [14], demonstrate high suppression effectiveness (82%) without energy consumption, resulting in theoretically infinite energy efficiency. However, their performance is fixed and nonadaptive, limiting practical use in dynamic tremor conditions.

Semi-active orthoses, represented by devices, such as Zahedi et al.'s soft exoskeleton [8] and the layer-jamming glove by Wanasinghe et al. [50], offer improved adaptability. Zahedi et al.'s [8] device achieves a 61.8% suppression ratio with a moderate weight of 255 g and minimal power consumption (1 W), providing an efficiency of about 61.8%/W. Wanasinghe et al.'s [50] glove is exceptionally lightweight (30 g) and yields a notable suppression ratio of 78.3%, but its vacuum-driven actuation consumes around 5 W, resulting in a relatively lower energy efficiency (15.7%/W).

Active control devices, such as the pneumatic artificial muscle glove by Skaramagkas et al. [51] and Zhou et al.'s [30] wearable tremor suppression glove (WTSG), achieve superior suppression

Authorized licensed use limited to: Queen Mary University of London. Downloaded on February 28,2026 at 20:34:18 UTC from IEEE Xplore. Restrictions apply.

This article has been accepted for inclusion in a future issue of this journal. Content is final as presented, with the exception of pagination.

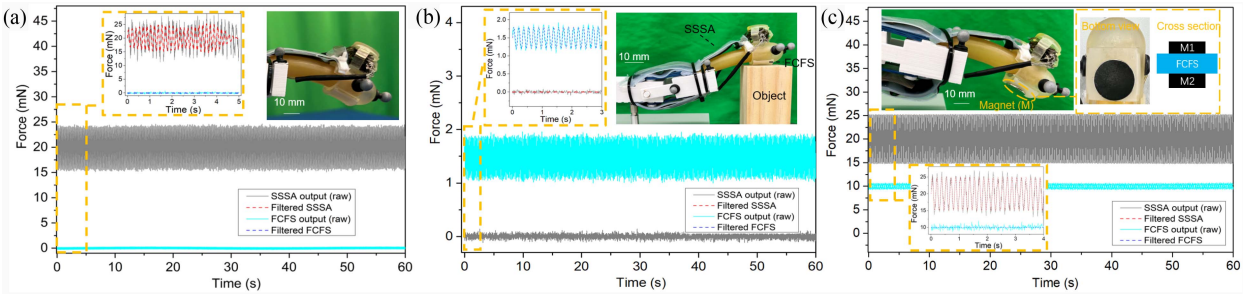

Fig. 10. Sensor outputs from the SSSA and FCFS under different finger tremor conditions: (a) resting tremor (no contact), (b) postural tremor with surface contact, and (c) kinetic tremor during object holding.

TABLE I
COMPARISON WITH OTHER HAND TREMOR SUPPRESSION ORTHOSES

Orthosis	Absorption	Substrate	Weight	Maximum suppression (%)	S/W (%/g)	Power (W)	E (%/W)
Passive Orthosis [14]	P	Flexible	33 g	82	2.48	0	∞
Soft glove [29]	A	Rigid	300 g	85	0.28	2.5–3	42–56
Soft exoskeleton [8]	S	Flexible	255 g	61.8	0.242	<1	61.8
Jamming glove [50]	S	Flexible	30 g	78.3	2.61	5	15.7
Pneumatic artificial muscle glove [51]	A	Rigid	280 g	75	0.27	6	12.5
Wearable tremor suppression device [30]	A	Rigid	580 g	85.5	0.147	6	14.3
WHTOG	S & A	Flexible	155 g	81.7	0.53	<0.5	163.4

P: passive; A: active; S: semiactive; S/W: the index of the suppression ratio in unit weight; the energy efficiency E is defined as the ratio between the maximum tremor suppression and the average power consumption: Maximum suppression (%) / Power (W).

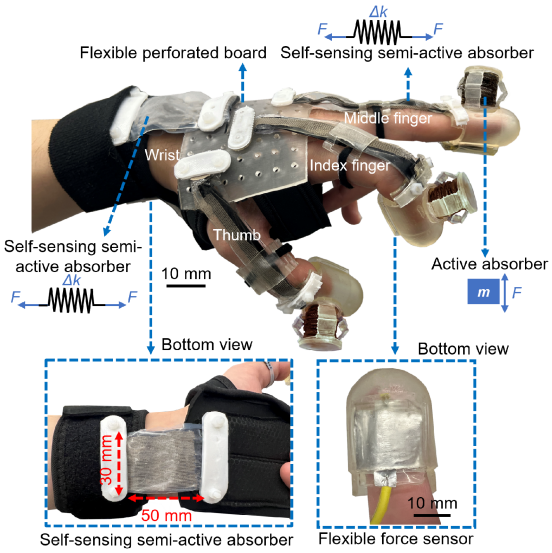

Fig. 11. Prototype of the WHTOG: a Velcro strap is used to secure the position of the two SSSAs on the wrist, while a flexible perforated board allows for adjusting their positions. In addition, small Velcro straps on the fingers are used to attach and secure the SSSAs to the fingers. Multiple layers of SSSAs are secured using 3D-printed thermoplastic polyurethane fixers with screws.

ratios of 75% and 85.5%, respectively. Nevertheless, these active systems are usually heavier (280–580 g) and have higher power demands (6 W), consequently exhibiting lower energy efficiencies of approximately 12.5 and 14.3%/W, respectively.

The proposed WHTOG uniquely integrates both semi-active and active control schemes, utilizing PVC gel-based actuators and flexible sensors. With a total weight of only 155 g, it provides a high suppression ratio of 81.7% at the fingertip. The system's total power consumption is carefully estimated based on the actual driving conditions, including three AFTAs (each containing 27 actuator units) and five SSSAs operating at a voltage of 700 V. Considering an average current draw of approximately 8 μA per AFTA unit (based on the typical ON–OFF modulation of the AFTA actuators during tremor cycles, the effective duty cycle was estimated to be below 40%) and around 10 μA per SSSA module, the total electrical power consumption of the system is conservatively estimated to remain below 0.5 W. More importantly, due to its low estimated power consumption, the WHTOG achieves an exceptionally high energy efficiency of approximately 163.4%/W. Such a combination of lightweight design, adaptability, high suppression performance, and superior energy efficiency distinctly positions the WHTOG ahead of other contemporary systems, especially for prolonged wearable applications where comfort and low power consumption are critical.

IV. CONCLUSION

This work presented a WHTOG that integrates semi-active and active control schemes through PVC gel-based actuators and flexible sensing elements. By combining SSSAs and active fingertip tremor absorbers (AFTAs), the system leverages the energy efficiency of semi-active damping and the precision of active vibration control within a compact, soft robotic framework. The incorporation of resistive strain and capacitive force sensors enables accurate detection of tremor signals under both

Authorized licensed use limited to: Queen Mary University of London. Downloaded on February 28,2026 at 20:34:18 UTC from IEEE Xplore. Restrictions apply.

This article has been accepted for inclusion in a future issue of this journal. Content is final as presented, with the exception of pagination.

free-space and contact conditions, ensuring robust performance across diverse scenarios.

Dynamic simulations and experimental evaluations confirmed that the proposed glove can effectively suppress tremors over a broad frequency range of 3–12 Hz. Semi-active damping achieved up to 72% reduction at the palm and 71.6% at the fingertips, while the addition of active control further improved fingertip suppression to 81.7%. The glove's lightweight design (155 g) and low power consumption (0.5 W) result in a high energy efficiency of 163.4%/W, outperforming most existing wearable orthoses. These results confirm the feasibility of the proposed hybrid actuation strategy for practical, long-term tremor suppression and demonstrate that hybrid actuation and sensing can jointly deliver both comfort and high performance.

In summary, the WHTOG advances the state of wearable tremor-suppression technologies by uniting adaptive actuation, integrated sensing, and low-power operation in a single system. This approach provides a promising foundation for next-generation soft robotic orthoses aimed at enhancing daily functionality and quality of life for individuals with hand tremors. Beyond tremor management, the presented concept may also inspire the development of other wearable robotic systems for motion assistance, rehabilitation, and human–robot interaction. Future work will focus on refining control coordination, validating the system in clinical settings, and extending the actuator–sensor bandwidth to experimentally assess performance beyond 12 Hz.

REFERENCES

[1] E. D. Louis and P. L. Faust, "Essential tremor pathology: Neurodegeneration and reorganization of neuronal connections," *Nature Rev. Neurol.*, vol. 16, no. 2, pp. 69–83, Jan. 2020.

[2] S. Paschen et al., "Long-term efficacy of deep brain stimulation for essential tremor: An observer-blinded study," *Neurol.*, vol. 92, no. 12, pp. e1378–e1386, May 2019.

[3] T. Welton et al., "Essential tremor," *Nature Rev. Dis. Primers*, vol. 7, no. 1, May 2021, Art. no. 83.

[4] M. N. Alam, B. Johnson, J. Gendreau, K. Tavakolian, C. Combs, and R. Fazel-Rezai, "Tremor quantification of Parkinson's disease-A pilot study," in *IEEE Int. Conf. Electro Inf. Technol. (EIT)*, Aug. 2016, pp. 755–759.

[5] T. Novak and K. M. Newell, "Physiological tremor (8–12 hz component) in isometric force control," *Neurosci. Lett.*, vol. 641, pp. 87–93, Feb. 2017.

[6] G. Deuschl, J. Raethjen, M. Lindemann, and P. Krack, "The pathophysiology of tremor," *Muscle Nerve: Official J. Amer. Assoc. Electrodiagnostic Med.*, vol. 24, no. 6, pp. 716–735, May 2001.

[7] C. R. Kelley and J. L. Kauffman, "Tremor-active controller for dielectric elastomer-based pathological tremor suppression," *IEEE/ASME Trans. Mechatron.*, vol. 25, no. 2, pp. 1143–1148, Apr. 2020.

[8] A. Zahedi, B. Zhang, A. Yi, and D. Zhang, "A soft exoskeleton for tremor suppression equipped with flexible semiactive actuator," *Soft Robot.*, vol. 8, no. 4, pp. 432–447, Aug. 2021.

[9] G. Wang, H. Wang, W. Gao, X. Yang, and Y. Wang, "Jamming enabled variable stiffness wrist exoskeleton for tremor suppression," *IEEE Robot. Automat. Lett.*, vol. 8, no. 6, pp. 3693–3700, Apr. 2023.

[10] A. Pascual-Valdunciel et al., "Peripheral electrical stimulation to reduce pathological tremor: A review," *J. neuroeng. Rehabil.*, vol. 18, pp. 1–19, Feb. 2021.

[11] A. Yi, A. Zahedi, Y. Wang, U.-X. Tan, and D. Zhang, "A novel exoskeleton system based on magnetorheological fluid for tremor suppression of wrist joints," in *IEEE 16th Int. Conf. Rehabil. Robot. (ICORR)*, Jul. 2019, pp. 1115–1120.

[12] W. Awantha, A. Wanasinghe, A. Kavindya, A. Kulasekera, and D. Chathuranga, "A novel soft glove for hand tremor suppression: Evaluation of layer jamming actuator placement," in *3rd IEEE Int. Conf. soft Robot. (RoboSoft)*, Jun. 2020, pp. 440–445.

[13] E. Buki, R. Katz, M. Zacksenhouse, and I. Schlesinger, "Vib-bracelet: A passive absorber for attenuating forearm tremor," *Med. Biol. Eng. Comput.*, vol. 56, pp. 923–930, May 2018.

[14] N. P. Fromme, M. Camenzind, R. Riener, and R. M. Rossi, "Design of a lightweight passive orthosis for tremor suppression," *J. Neuroeng. Rehabil.*, vol. 17, pp. 1–15, Apr. 2020.

[15] M. Aliff, M. A. Dinie, I. Yusof, and N. Sani, "Development of smart glove rehabilitation device (SGRD) for Parkinson's disease," *Int. J. Innov. Technol. Exploring Eng. (IJITEE)*, vol. 9, no. 2, pp. 4512–4518, Dec. 2019.

[16] J. Wirekoh, N. Parody, C. N. Riviere, and Y.-L. Park, "Design of fiber-reinforced soft bending pneumatic artificial muscles for wearable tremor suppression devices," *Smart Mater. Structures*, vol. 30, no. 1, Dec. 2020, Art. no. 015013.

[17] C. Liu and K. Zhang, "A wearable finger tremor-suppression orthosis using the pvc gel linear actuator," *IEEE Robot. Autom. Lett.*, vol. 9, no. 4, pp. 3854–3861, Feb. 2024.

[18] Y. Wang, X.-J. Liu, and H. Zhao, "Control and implementation of a fluidic elastomer actuator for active suppression of hand tremor," *IEEE Robot. Autom. Lett.*, vol. 9, no. 2, pp. 939–946, Dec. 2023.

[19] Z. Zhu, Z. Wang, K. Dai, X. Wang, H. Zhang, and W. Zhang, "An adaptive and space-energy efficiency vibration absorber system using a self-sensing and tunable magnetorheological elastomer," *Nano Energy*, vol. 117, Dec. 2023, Art. no. 108927.

[20] D. Kim and R. B. Gillespie, "Origami structured compliant actuator (OSCA)," in *2015 IEEE Int. Conf. Rehabil. Robot. (ICORR)*, Oct. 2015, pp. 259–264.

[21] C. Liu, J. J. Busfield, and K. Zhang, "An electric self-sensing and variable-stiffness artificial muscle," *Adv. Intell. Syst.*, Jul. 2023, Art. no. 2300131.

[22] C. Liu, M. H. Uddin, and K. Zhang, "Capacitive pvc gel pressure sensors with various interlinked microstructural dielectric middle layers," *Sensors Actuators A: Phys.*, 2024, Art. no. 115519.

[23] B. Widrow, J. McCool, and M. Ball, "The complex LMS algorithm," *Proc. IEEE*, vol. 63, no. 4, pp. 719–720, Apr. 1975.

[24] Z. Li, M. Sheng, M. Wang, P. Dong, B. Li, and H. Chen, "Stacked dielectric elastomer actuator (SDEA): Casting process, modeling and active vibration isolation," *Smart Mater. Structures*, vol. 27, no. 7, Jun. 2018, Art. no. p. 0 75023.

[25] C. Zhou, H. Zou, and X. Qiu, "A frequency band constrained filtered–x least mean square algorithm for feedback active control systems," *J. Acoustical Soc. America*, vol. 148, no. 4, pp. 1947–1951, Oct. 2020.

[26] R. S. A. Araújo et al., "Analysis of adaptive algorithms based on least mean square applied to hand tremor suppression control," *Appl. Sci.*, vol. 13, no. 5, Mar. 2023, Art. no. 3199.

[27] N. Ogawa, M. Hashimoto, M. Takasaki, and T. Hirai, "Characteristics evaluation of pvc gel actuators," in *IEEE/RSJ Int. Conf. Intell. Robots Syst*, 2009, pp. 2898–2903.

[28] Y. Li and M. Hashimoto, "PVC gel based artificial muscles: Characterizations and actuation modular constructions," *Sensors Actuators A: Phys.*, vol. 233, pp. 246–258, Sep. 2015.

[29] Y. Zhou, M. E. Jenkins, M. D. Naish, and A. L. Trejos, "Development of a wearable tremor suppression glove," in *7th IEEE Int. Conf. Biomed. Robot. Biomechatronics (Biorob)*, 2018, pp. 640–645.

[30] Y. Zhou, A. Ibrahim, K. G. Hardy, M. E. Jenkins, M. D. Naish, and A. L. Trejos, "Design and preliminary performance assessment of a wearable tremor suppression glove," *IEEE Trans. Biomed. Eng.*, vol. 68, no. 9, pp. 2846–2857, Sep. 2021.

[31] Y. Li, Y. Li, and M. Hashimoto, "Low-voltage planar PVC gel actuator with high performances," *Sensors Actuators B: Chem.*, vol. 282, pp. 482–489, Mar. 2019.

[32] M. Hashimoto, "Development of an artificial muscle using PVC gel," in *ASME Int. Mech. Eng. Congr. Expo.*, vol. 54884, pp. 745–754, 2011.

[33] S. Komandur, P. W. Johnson, R. L. Storch, and M. G. Yost, "Relation between index finger width and hand width anthropometric measures," in *2009 Annu. Int. Conf. IEEE Eng. Med. Biol. Soc.*, 2009, pp. 823–826.

[34] C. W. Hess and S. L. Pullman, "Tremor: Clinical phenomenology and assessment techniques," *Tremor Other Hyperkinetic Movements*, vol. 2, pp. 1–15, Jun. 2012, Art. no. tre-02-65-365-1.

[35] R. J. Elble, "Tremor: Clinical features, pathophysiology, and treatment," *Neurologic Clin.*, vol. 27, no. 3, pp. 679–695, Aug. 2009.

Authorized licensed use limited to: Queen Mary University of London. Downloaded on February 28,2026 at 20:34:18 UTC from IEEE Xplore. Restrictions apply.

This article has been accepted for inclusion in a future issue of this journal. Content is final as presented, with the exception of pagination.

[36] F. Budini, L. Labanca, M. Scholz, and A. Macaluso, "Tremor, finger and hand dexterity and force steadiness, do not change after mental fatigue in healthy humans," *Plos one*, vol. 17, no. 8, 2022, Art. no. e0272033.
[37] D. E. Vaillancourt, A. B. Slifkin, and K. M. Newell, "Regularity of force tremor in Parkinson's disease," *Clin. Neuriophysiol.*, vol. 112, no. 9, pp. 1594–1603, Sep. 2001.
[38] D. J. Inman, *Vibration With Control*. West Sussex, U.K.: Wiley, 2017.
[39] S. Kazi, M. Mailah, and Z. Zain, "Suppression of hand postural tremor via active force control method," *Manuf. Eng. Autom. Control Robot*, vol. 2023, no. 20, 2014, Art. no. 129.
[40] D. Formica, S. K. Charles, L. Zollo, E. Guglielmelli, N. Hogan, and H. I. Krebs, "The passive stiffness of the wrist and forearm," *J. Neuriophysiol.*, vol. 108, no. 4, pp. 1158–1166, 2012.
[41] T. Gupta, "Identification and experimental validation of damping ratios of different human body segments through anthropometric vibratory model in standing posture," *asmedigitalcollection*, vol. 129, no. 4, pp. 556–574, Aug. 2007.
[42] Y. Wu et al., "A bioinspired multi-knuckle dexterous pneumatic soft finger," *Sensors Actuators A: Phys.*, vol. 350, Feb. 2023, Art. no. 114105.
[43] N. Sharma and M. Venkadesan, "Finger stability in precision grips," *Proc. Nat. Acad. Sci.*, vol. 119, no. 12, Mar. 2022, Art. no. e2122903119.
[44] J. Park, N. Pažin, J. Friedman, V. M. Zatsiorsky, and M. L. Latash, "Mechanical properties of the human hand digits: Age-related differences," *Clin. Biomech.*, vol. 29, no. 2, pp. 129–137, Feb. 2014.
[45] Y. Zhou, M. E. Jenkins, M. D. Naish, and A. L. Trejos, "The measurement and analysis of parkinsonian hand tremor," in *IEEE-EMBS Int. Conf. Biomed. Health Informat. (BHI)*, 2016, pp. 414–417.
[46] G. Grimaldi, M.-U. Manto, and M. Manto, *Tremor: From Pathogenesis to Treatment*, vol. 20. San Rafael, CA, US: Morgan & Claypool Publishers, 2008.
[47] J. S. Lora-Millan, G. Delgado-Oleas, J. Benito-León, and E. Rocon, "A review on wearable technologies for tremor suppression," *Front. Neurol.*, vol. 12, Aug. 2021, Art. no. 700600.
[48] B. Taheri, D. Case, and E. Richer, "Adaptive suppression of severe pathological tremor by torque estimation method," *IEEE/ASME Trans. Mechatron.*, vol. 20, no. 2, pp. 717–727, May 2014.
[49] V. Skaramagkas, G. Andrikopoulos, Z. Kefalopoulou, and P. Polychronopoulos, "A study on the essential and Parkinson's arm tremor classification," *Signals*, vol. 2, no. 2, pp. 201–224, Apr. 2021.
[50] A. Wanasinghe, W. Awantha, A. Kavindya, A. Kulasekera, D. Chathuranga, and B. Senanayake, "A layer jamming soft glove for hand tremor suppression," *IEEE Trans. Neural Syst. Rehabil. Eng.*, vol. 29, pp. 2684–2694, Dec. 2021.
[51] V. Skaramagkas, G. Andrikopoulos, and S. Manesis, "An experimental investigation of essential hand tremor suppression via a soft exoskeletal glove," in *Eur. Control Conf. (ECC)*, Jul. 2020, pp. 889–894.



Chen Liu received the Ph.D. degree in mechanical engineering in 2024 from the Queen Mary University of London, London, U.K., where he focused on the development of wearable devices and soft robotic systems for medical applications.

He subsequently held a Research Fellow position with University College London (UCL), affiliated with the Hawkes Institute, the Robotics Institute, and the Centre for Medical Image Computing. He is currently a Research Associate with the Bristol Robotics Laboratory, University of Bristol, Bristol, U.K. His research interests include soft robotics and medical robotics, with an emphasis on the design, fabrication, and control of soft robotic systems for healthcare, surgical, and human-assistive applications.



Yan Wang received the B.Eng. degree in mechanical design, manufacture and automation from the North University of China, Taiyuan, China, and the M.Sc. degree in mechanical engineering, and the Ph.D. degree in mechanical engineering from the Queen Mary University of London, London, U.K., in 2017, 2019, and 2025, repectively.

His research primarily focuses on the design and control of multirotor UAVs, particularly those with reconfigurable and deployable mechanisms that enable geometric size changes. In addition, he develops control strategies to ensure safe flight operations.



Ketao Zhang (Member, IEEE) received the Ph.D. degree in mechanical engineering through a joint program from King's College London, London, U.K., in 2011, and Beijing Jiaotong University, Beijing, China.

He is currently a Reader within the Centre for Advanced Robotics, Queen Mary University of London, London. He is an author of more than 100 peer-reviewed papers. His research interests include the design theory of robot mechanisms and manipulators, robotic manipulation, soft robotics, aerial robotics, and their applications in manufacturing, assistive devices, and inspection in challenging environments.

Dr. Zhang was the recipient of the Howard Medal presented by ICE. He is currently an Associate Editor for IEEE ROBOTICS AND AUTOMATION LETTERS, *ASME Journal of Mechanical Design*, and *Mechanism and Machine Theory*.

Authorized licensed use limited to: Queen Mary University of London. Downloaded on February 28,2026 at 20:34:18 UTC from IEEE Xplore. Restrictions apply.